GEOPHYSICAL RESEARCH LETTERS, VOL. 40, 4777–4782, doi:10.1002/grl.50910, 2013

Mechanism of column and carrot sprites derived from optical and radio observations

Jianqi Qin,[1] Sebastien Celestin,[2] Victor P. Pasko,[1] Steven A. Cummer,[3]
Matthew G. McHarg,[4] and Hans C. Stenbaek-Nielsen[5]

Received 5 August 2013; accepted 23 August 2013; published 12 September 2013.

[1] The lightning current waveforms observed simultaneously with high-speed video records of a column and a carrot sprite event are incorporated in a plasma fluid model to provide quantitative explanation of these two distinct morphological classes of transient luminous events. We calculate the strength of the lightning-induced electric field at sprite altitudes using a time integral of the ionization frequency $\int_0^t \nu_i(E/N)\mathrm{d}t$. For the studied two events, modeling results indicate that these integral values never exceed 18 in the lower ionosphere, which is the minimum value required for the initiation of streamers from single seed electrons according to the Raether-Meek criterion. It is therefore suggested that the presence of electron inhomogeneities is a necessary condition for the initiation of sprite streamers. It is further demonstrated using streamer modeling that a minimum value of the integral ∼10 is necessary to initiate upward negative streamers from inhomogeneities, corresponding to a minimum charge moment change of ∼500 C km under typical nighttime conditions. If the integral values in the entire upper atmosphere are smaller than ∼10, only column sprites can be produced, dominated by downward positive streamers. **Citation:** Qin, J., S. Celestin, V. P. Pasko, S. A. Cummer, M. G. McHarg, and H. C. Stenbaek-Nielsen (2013), Mechanism of column and carrot sprites derived from optical and radio observations, *Geophys. Res. Lett.*, *40*, 4777–4782, doi:10.1002/grl.50910.

1. Introduction

[2] Sprites are large-scale luminous gas discharges in the upper atmosphere that exhibit a variety of morphologies resembling straight columns, carrots, jellyfish, or fireworks in normal-rate (≲1000 fps) video observations [e.g., *Stenbaek-Nielsen et al.*, 2000; *Pasko et al.*, 2011; *Bor*, 2013]. In higher-speed (≳5000 fps) video observations, the morphological complexity of sprites is manifested as the significant variation of halo luminosity, the absence or presence of upward negative streamers, and the complicated initiation sequence of downward and upward streamers [e.g., *Cummer et al.*, 2006; *McHarg et al.*, 2007; *Stenbaek-Nielsen and McHarg*, 2008]. Simultaneous observations of sprites and ELF/VLF sferics suggest that the morphological features of sprites are closely related to the characteristics of their causative positive cloud-to-ground lightning discharges (+CGs) [e.g., *Wescott et al.*, 1998; *van der Velde et al.*, 2006; *Suzuki et al.*, 2011]. Observations of "negative sprites" (produced by –CGs) lend further support to the dependence of sprite morphology on lightning characteristics, showing that all negative sprites have similar morphological features, in accordance with the similarity of the characteristics of their causative –CGs [*Li et al.*, 2012].

[3] Recent modeling studies provide a testable theory for understanding of the origin of different sprite morphologies [*Qin et al.*, 2012a, 2013]. In that theory, column sprites, characterized by predominantly vertical downward streamers, and carrot sprites, exhibiting both upward and downward propagating streamers, are, respectively, produced by +CGs associated with charge moment changes smaller and larger than a threshold of ∼500 C km under typical nighttime conditions. For a sufficiently large charge moment change capable of producing carrot sprites, the specific shape of the carrot sprites (e.g., the luminosity of the halo, the size and brightness of the upper diffuse region) is determined by the time dynamics of the charge moment changes (i.e., the rise time, peak current, and the strength of the continuing current) [*Qin et al.*, 2013]. In the present work, the lightning current moment waveforms observed simultaneously with a column and a carrot sprite events are incorporated into a plasma fluid model with the goal to subject the above-mentioned theory to a quantitative test by comparing the morphological features predicted by the model with those appearing in video observations.

2. Observations

[4] Since we are specifically interested in comparing sprite observations with streamer modeling to understand the fundamental physics related to different sprite morphologies rather than conducting a statistical analysis on the lightning characteristics producing sprites with different morphologies, in the present work, we numerically simulate only one column and one carrot sprite event, recorded, respectively, on 15 July 2010 and 20 July 2012 using a 12,500 fps camera. Figure 1 shows six images of the column sprite event with a time interval of 0.24 ms in the

[1]Communications and Space Sciences Laboratory, Department of Electrical Engineering, Pennsylvania State University, University Park, Pennsylvania, USA.
[2]Laboratory of Physics and Chemistry of the Environment and Space, National Center for Scientific Research, Observatory of Sciences of the Universe in the French Center region, University of Orleans, Orleans, France.
[3]Electrical and Computer Engineering Department, Pratt School of Engineering, Duke University, Durham, North Carolina, USA.
[4]Department of Physics, United States Air Force Academy, Colorado Springs, Colorado, USA.
[5]Geophysical Institute, University of Alaska Fairbanks, Fairbanks, Alaska, USA.

Corresponding author: J. Qin, Communications and Space Sciences Laboratory, Department of Electrical Engineering, Pennsylvania State University, 227 Electrical Engineering East, University Park, PA 16802-2706, USA. (jianqiqin@psu.edu)

0094-8276/13/10.1002/grl.50910

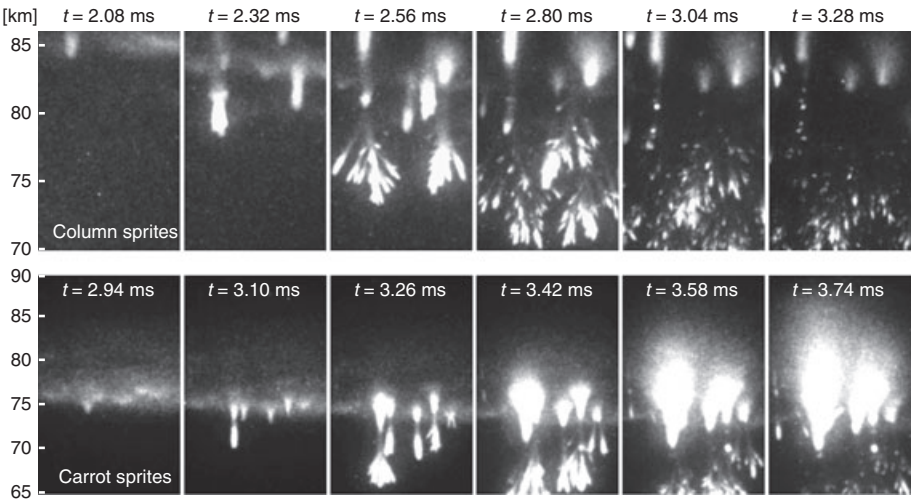

Figure 1. Image series of (top) a column sprite event observed on 15 July 2010 and of (bottom) a carrot sprite event observed on 20 July 2012, each labeled with its time from the onset of the related lightning return stroke.

top panels and six of the carrot sprite event with a time interval of 0.16 ms in the bottom panels. The most significant difference of these two events in terms of their morphologies is that in the carrot sprite event, an extensive upper diffuse region formed by upward propagating negative streamers is present, whereas in the column sprite event, only small and fuzzy luminous structures around the origins of the downward propagating streamers are perceptible but insufficient to create an obvious carrot characteristics, similar to those discussed by *Stenbaek-Nielsen and McHarg* [2008]. By contrast, the dynamics of the downward positive streamers in these two events are almost identical, both showing clear processes of streamer propagation, brightening, and branching as well as some bright spots near the location of streamer branching. Therefore, it is essential to investigate the initiation and propagation of the upward negative streamers in order to understand the origin of different sprite morphologies.

[5] The reason why we choose these two particular events for analysis rather than many others available in our database is because their causative +CGs were temporarily isolated. For both events, there is no National Lightning Detection Network-reported flash or stroke within 200 km in the 2 s period before the sprite-producing stroke. The ULF data confirm that there is no unreported stroke that produced detectable continuing current during the same preceding 2 s period. This prevents any possible contributions from, if present, the lightning events that occurred prior to the ones directly responsible for the sprites. Figure 2 shows the lightning current waveforms extracted by deconvolving the observed ELF sferic waveforms with a modeled ELF impulse response, employing methodology similar to that used by *Cummer and Inan* [1997]. The return stroke of the +CG responsible for the column sprite event has a large peak current moment of ∼1230 kA km and a short duration of ∼0.8 ms, producing a charge moment change of ∼406.0 C km in 0.8 ms and followed by weak continuing current associated with ∼52.7 C km in 4.2 ms (i.e., total 458.7 C km in first 5 ms). The return stroke of the +CG related to the carrot sprites has a smaller peak current moment of ∼738.7 kA km and a longer duration of ∼1.5 ms, producing ∼564.9 C km charge moment change and followed by stronger continuing current associated with 92.6 C km charge moment change in ∼3.5 ms (i.e., total 657.5 C km in first 5 ms).

3. Model

[6] A two-dimensional cylindrically symmetric (*r*, *z* dependent) plasma fluid model developed by *Qin et al.* [2013] is used to simulate the time dynamics of sprite halos and sprite streamers. In this model, the chemical reactions accounted for include electron impact ionization of N_2 and O_2, electron dissociative attachment to O_2, and the electron detachment process $O^-+N_2 \rightarrow e+N_2O$ [*Qin et al.*, 2013, equation (1)–(4)]. Photoionization processes are included using the three-group SP_3 model developed by *Bourdon et al.* [2007]. The motion of charged species is simulated by solving the drift-diffusion equations for electrons and ions coupled with Poisson's equation [e.g., *Qin et al.*, 2013, equation (5)–(9)]. The transport equations for charged species are solved using a flux-corrected transport technique

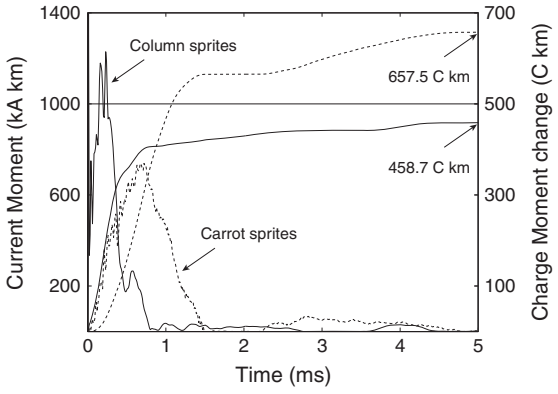

Figure 2. Current waveforms of the +CGs producing (solid) the column sprite event on 15 July 2010 starting at 07:06:09:808 880 UT and (dashed) the carrot sprite event on 20 July 2012 starting at 06:27:17:157 860 UT. The charge moment changes illustrated by right vertical axis are obtained by integrating the current moments over time.

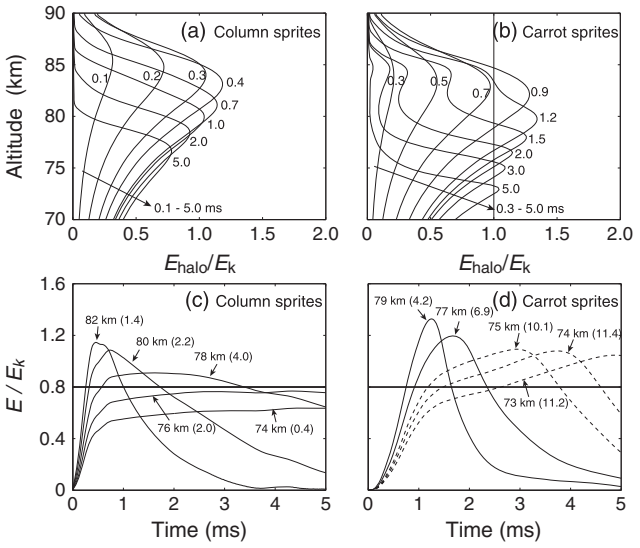

Figure 3. (a, b) Spatial variation of the reduced electric field E_{halo}/E_k along the axis of symmetry of the halo at different moments of time, respectively, in the column and carrot sprite events. (c, d) Temporal variation of the reduced electric field along the axis of symmetry of the halo at different altitudes, respectively, in the column and carrot sprite events. Dashed lines in Figure 3d correspond to the altitudes at which upward negative streamers can be initiated. The column event starts at 07:06:09:808 880 UT on 15 July 2010, and the carrot event starts at 06:27:17:157 860 UT on 20 July 2012. The numbers in parentheses represent the αd values obtained by integrating ν_i as a function of E/N in the 5 ms timescale at each altitude.

[*Zalesak*, 1979] that combines an eighth-order scheme for the high-order fluxes and a donor cell scheme for the low-order fluxes. The profile of the ambient ionospheric electron density n_e is expressed as follows [*Wait and Spies*, 1964]:

$$n_e(h) = 1.43 \times 10^{13} e^{-0.15h'} e^{(\beta-0.15)(h-h')} [m^{-3}] \quad (1)$$

where h' (in kilometers) and β (in km^{-1}) are given parameters describing reference altitude and sharpness, respectively, and h is the altitude of interest. In the present work, we choose $h' = 85$ km and $\beta = 0.5$ km^{-1} to represent typical nighttime conditions [*Han and Cummer*, 2010]. The ambient positive ion density equals the electron density at high altitudes where electron density is higher than 10^8 m^{-3}, and is 10^8 m^{-3} at low altitudes [e.g., *Qin et al.*, 2013]. The ambient negative ion density is then calculated based on charge neutrality. The drift of ions is incorporated assuming the mobility of ions as a function of altitude $\mu_i \simeq 2.3 N_0/N$ cm^2/V/s [*Davies*, 1983], where N is the air density at altitude of interest and $N_0 \simeq 2.688 \times 10^{25}$ m^{-3} is its reference value at ground level.

[7] A two-step simulation technique proposed by *Qin et al.* [2012a] is used to model the initiation of streamers during the development of the halo. In the first step, we model the large-scale halo dynamics in a simulation domain that extends from the ground up to 95 km, with a radius of 95 km and perfectly conducting boundary conditions on the upper (ionosphere), lower (ground), and lateral (95 km away from the center) boundaries using a numerical grid with a spatial resolution of 237.5 m. We keep track of the electric field $\vec{E}_{halo}(r, z, t)$ in the upper atmosphere during this step, and then use this field as an externally applied electric field during the second step to model possible small-scale sprite streamer initiation using a much finer numerical grid. The simulation domain in the second step extends 2 km vertically and has a radius of 0.25 km with open boundary conditions [*Liu and Pasko*, 2006], and it is discretized using grids with 3201 × 401 grid points, corresponding to a spatial resolution of 0.625 m. The variation of air density with altitude is accounted for, and the initial electron and ion densities in the streamer simulation domain are the same as those in the corresponding region in sprite halo modeling, defined by the equation (1). To model the streamer initiation, we place a test inhomogeneity at different altitudes on the axis of the halo and use a streamer model to simulate its evolution under application of $\vec{E}_{halo}(r, z, t)$. The test inhomogeneities have Gaussian density distributions:

$$n_{inhomo} = n_{peak} \exp\left[-\frac{r^2}{r_0^2} - \frac{(z-h_0)^2}{z_0^2}\right] \quad (2)$$

where h_0, n_{peak}, r_0, and z_0 are the altitude, the peak density, and the characteristic size of the inhomogeneity in radial and axial directions, respectively. In the present study, $n_{peak} = 2 \times 10^9$ m^{-3} and $r_0 = z_0 = 30$ m, identical to those used by *Qin et al.* [2013]. We note that the chosen inhomogeneity is the most optimal for initiation of streamers [*Qin et al.*, 2013, and extensive discussion therein] and allows careful quantitative description of differences in initiation of sprites and their morphology for experimentally specified current/charge moment dynamics, which represents the goal of the present study.

4. Results

[8] In the first modeling step, we simulate the halo dynamics to investigate the variation of the large-scale lightning electric field in the upper atmosphere. Figure 3 shows the reduced electric field (i.e., E_{halo}/E_k) on the axis of symmetry of the halo in two different ways: Figures 3a and 3b show the spatial variation of the reduced electric field at different moments of time, whereas Figures 3c and 3d show the temporal variation of the reduced electric field at different altitudes. Comparing these spatial and temporal variations of the reduced electric fields calculated using experimentally measured lightning current waveforms with theoretical results presented by *Qin et al.* [2013], we see that the electric fields shown in Figure 3a are very similar to those shown by *Qin et al.* [2013, Figure 4b] that are predicted to produce column sprites, and the electric fields shown in Figure 3b are similar to those shown by *Qin et al.* [2013, Figure 6b] that are suggested to produce carrot sprites. A critical difference in the dynamics of the reduced electric fields shown in Figure 3 is that in the carrot sprite event, there is a large region below ∼76 km altitude (i.e., at 75, 74, 73 km and lower altitudes) where the electric field exceeds $0.8E_k$ with a peak value of $\sim 1.2E_k$, and persists for longer than ∼2 ms, whereas in the column sprite event, only at ∼78 km altitude, the electric field slightly exceeds $0.8E_k$ and persists for ∼2 ms.

[9] An electric field that exceeds $0.8E_k$ and persists for $\gtrsim$2 ms is a requirement to initiate upward negative streamers at typical sprite altitudes (∼75 km) according to the analysis of *Qin et al.* [2013]. This criterion is approximate because at different altitudes, the timescale required for streamer

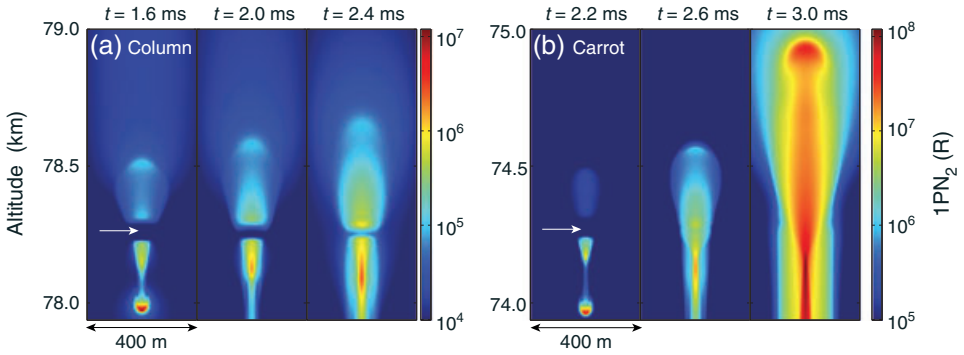

Figure 4. Cross-sectional view of optical emissions on the axis of symmetry for a streamer produced (a) in the column sprite event and (b) in the carrot sprite event. Each frame is labeled with its time from the onset of the related lightning return stroke. The arrows point to the initial position of the inhomogeneities.

initiation, which is inversely proportional to the air density [*Pasko et al.*, 1998], could be significantly different. This means that at different altitudes, an electric field of $0.8E_k$ that lasts for 2 ms leads to different αd values as discussed below. The ability of the lightning electric field to initiate streamers can be estimated more accurately using a single value (rather than a combination of its magnitude and persistence) by integrating the reduced electric field dependent ionization frequency $\nu_i(E/N)$ over time (i.e., $\int_0^t \nu_i(E/N)\mathrm{d}t$). This value is equivalent to the αd value in the Raether-Meek criterion in regard to the avalanche-to-streamer transition between two electrodes, which states that when an electron avalanche propagates a long enough distance d from the initial position of the primary electron so that the product of d and the ionization coefficient $\alpha(E/N)$ approaches a value of 18 (i.e., $\alpha d \simeq 18$), the electron avalanche will transform into a streamer [*Raizer*, 1991, section 12.2.5, p. 332]. For a given reduced electric field, the ionization coefficient α scales with altitude as N, whereas d scales as $1/N$ so that the criterion $\alpha d \simeq 18$ can be used as an approximation at sprite altitudes. We note that when the problem can be considered as purely local with α only dependent on time [*Qin et al.*, 2011], which is true in all simulations in the present work, the quantity $\int_0^t \nu_i \mathrm{d}t = \int_0^t \alpha v_e \mathrm{d}t$, where v_e is the electron drift velocity, effectively carries the same meaning as αd in the original Raether-Meek criterion. Hereafter, for convenience $\int_0^t \nu_i(E/N)\mathrm{d}t$ is referred to as the αd value. The value $e^{\alpha d}$ (i.e., $e^{\int_0^t \nu_i(E/N)\mathrm{d}t}$) represents the total number of free electrons produced by a single seed electron through ionization under the application of an electric field E with a duration of t. The numbers in parentheses in Figures 3c and 3d represent the αd values obtained by integrating ν_i as a function of E/N [*Morrow and Lowke*, 1997] over the 5 ms time interval at each altitude.

[10] In the second modeling step, we place a test inhomogeneity at different altitudes and apply the spatially and temporally varying electric field obtained in the first modeling step (see Figure 3) to model the initiation of streamers. In the column sprite event, we find that streamers cannot be initiated above 80 km altitude, and downward positive streamers can be initiated from inhomogeneities placed below 80 km down to 74 km altitude by the end of our 5 ms simulations. Note that downward positive streamers may also be able to initiate at altitudes lower than 74 km but with a delay longer than 5 ms. Figure 4a shows the streamer initiation from a test inhomogeneity placed at 78.25 km altitude, at which upward negative streamers have the best chance to be initiated since the αd value at this altitude is the largest according to the results shown in Figure 3c. Nevertheless, we see in Figure 4a that the upward luminous structure decays quickly and no negative streamer can be launched, which indicates that an electric field with $\alpha d = 4.0$ is not strong enough to initiate negative streamers. We emphasize that according to streamer simulations similar to those shown in Figure 4a, upward negative streamers cannot be initiated at any other altitudes with αd values even smaller than 4.0 in the column sprite event. A similar parametric study has also been conducted for the carrot sprite event, for which downward positive streamers are found to be able to initiate below 78 km altitude and upward negative streamers below 76 km altitude. It appears that the magnitude and persistence of the electric fields at 75, 74, and 73 km altitudes, which correspond to αd values of $\gtrsim 10$ (see Figure 3d), are enough for the initiation of negative streamers. Figure 4b shows the initiation of an upward negative streamer from an inhomogeneity placed at 74.25 km altitude. We note that the simulation domains for streamer initiation extend 2 km vertically (i.e., 77–79 km in Figure 4a and 73–75 km in Figure 4b). We show in Figure 4 only the streamer dynamics in the upper part of the simulation domain because the downward positive streamer initiates earlier and becomes very bright when the upward negative streamer initiates. The upward structure cannot be seen clearly when the entire domain is shown using common color scale. We also note that the downward positive streamers in the two cases have almost identical dynamics, both experience significant acceleration and exponential growth, similar to those modeled by *Liu et al.* [2009] and *Qin et al.* [2012a] and in good agreement with the similarity of the experimentally observed downward streamers shown in Figure 1.

5. Discussion

[11] *Qin et al.* [2013] theoretically studied the dependence of sprite morphology on lightning characteristics and concluded that column sprites and carrot sprites are, respectively, produced by +CGs associated with charge moment changes smaller and larger than a threshold of ~500 C km under typical nighttime conditions (i.e., the same ambient conditions as those used in the present study). A large charge

moment change can produce a strong electric field at low altitude where the ambient conductivity is low so that the electric field can persist above $0.8E_k$ for longer than ~2 ms, which is an empirical minimum requirement for the initiation of upward negative streamers [*Qin et al.*, 2013]. Therefore, statistically, the onset altitude of column sprites should be higher than that of carrot sprites [*Qin et al.*, 2013], in agreement with the observations of *Stenbaek-Nielsen et al.* [2010]. The simulation results obtained using experimentally observed lightning current waveforms in comparison with high-speed video observations in the present study support the conclusions of *Qin et al.* [2013].

[12] We have proposed a more accurate approach using the αd value in the Raether-Meek criterion to estimate the strength of the electric field at sprite altitudes. One important fact is that at none of the altitudes in either event, the αd value exceeds 18, which is the minimum αd value required for the initiation of positive and negative streamers from single seed electrons. This indicates that electron inhomogeneities in the lower ionosphere are necessary to initiate sprite streamers, as has been emphasized by *Qin et al.* [2011], and it is also why we assume the existence of such inhomogeneities in the first place. The polarization of those inhomogeneities produces strong space charge field in a localized region and therefore greatly facilitates the initiation of positive streamers by reducing the requirement of the αd value to as small as 0.4 if the electric field persists long enough (see Figure 3c). However, the initiation of negative streamers still requires a minimum αd value of ~10 (see Figure 3d). This is because the polarization of the inhomogeneity can lead to a more compact space charge distribution around its positive head than that in its negative head due to the fact that electrons are much more mobile than ions [*Qin et al.*, 2012b]. We note that the existence of such inhomogeneities in the lower ionosphere has not yet been demonstrated experimentally. Based on the above discussion, we see that an αd value of ~10 can be used as estimate of the minimum requirement for the initiation of upward negative streamers in sprite events. In other words, if the αd values in the entire upper atmosphere are smaller than 10, only column sprites can be produced. Note that the initiation mechanism of negative sprite streamers discussed above, which shows that the strength of ambient electric field needs to be large enough to initiate negative streamers, is different from the mechanism related to the negative charging in the positive streamer trail facilitating emergence of upward negative streamers suggested by *Luque and Ebert* [2010] and *Kosar et al.* [2012].

[13] It should be emphasized that the ambient conductivity in the lower ionosphere affects the threshold charge moment change producing carrot sprites, and under typical nighttime conditions, a minimum of ~500 C km is required [*Qin et al.*, 2013]. It appears that the charge moment changes producing the two events in the present study (respectively, 458.7 C km and 657.5 C km) agree with this threshold. This implies that the ambient conditions at the moments of these two events were close to the typical nighttime conditions (i.e., $h' = 85$ km and $\beta = 0.5$ km^{-1} in equation (1) [*Han and Cummer*, 2010]). In principle, variation of the threshold charge moment changes producing carrot sprites observed at different nights can be used as an indicator of the short-term or long-term variation of the lower ionospheric ambient conductivity.

[14] We finally summarize specific requirements needed for the formation of carrot sprites. We first note that the ambient electron density in the lower ionosphere decreases exponentially with decreasing altitude so that the lightning electric field can persist longer at lower altitudes. Moreover, a larger lightning charge moment change leads to larger electric fields at sprite altitudes. In a sprite event, if the causative lightning discharge produces a large charge moment change ($\gtrsim$500 C km under typical nighttime conditions), the lightning electric field can exceed $0.8E_k$ at low altitudes where the electric field can persist for longer than ~2 ms. In such a case, the lightning electric field at those low altitudes could have a large strength leading to $\alpha d \gtrsim 10$ so that upward negative streamers can be initiated, forming the upper region characteristics of a carrot sprite.

[15] **Acknowledgments.** This research was supported by the NSF Physical and Dynamic Meteorology and the Aeronomy Programs under grants AGS-0734083, ATM-1104441, ATM-0737605, ATM-0737294 and by the DARPA NIMBUS grants HR0011-101-0059. Sebastien Celestin's research was supported by the French space agency (CNES).

[16] The Editor thanks two anonymous reviewers for their assistance in evaluating this paper.

References

Bor, J. (2013), Optically perceptible characteristics of sprites observed in central Europe in 2007–2009, *J. Atmos. Sol.-Terr. Phys.*, *92*, 151–177, doi:10.1016/j.jastp.2012.10.008.

Bourdon, A., V. P. Pasko, N. Y. Liu, S. Celestin, P. Segur, and E. Marode (2007), Efficient models for photoionization produced by non-thermal gas discharges in air based on radiative transfer and the Helmholtz equations, *Plasma Sources Sci. Technol.*, *16*, 656–678.

Cummer, S. A., and U. S. Inan (1997), Measurement of charge transfer in sprite-producing lightning using elf radio atmospherics, *Geophys. Res. Lett.*, *24*, 1731–1734, doi:10.1029/97GL51791.

Cummer, S. A., N. C. Jaugey, J. B. Li, W. A. Lyons, T. E. Nelson, and E. A. Gerken (2006), Submillisecond imaging of sprite development and structure, *Geophys. Res. Lett.*, *33*, L04104, doi:10.1029/2005GL024969.

Davies, D. K. (1983), Measurements of swarm parameters in dry air, in *Theoretical Notes, Note 346*, edited by Westinghouse R&D Center, Pittsburgh, PA.

Han, F., and S. A. Cummer (2010), Midlatitude nighttime D region ionosphere variability on hourly to monthly time scales, *J. Geophys. Res.*, *115*, A09323, doi:10.1029/2010JA015437.

Kosar, B. C., N. Liu, and H. K. Rassoul (2012), Luminosity and propagation characteristics of sprite streamers initiated from small ionospheric disturbances at sub-breakdown conditions, *J. Geophys. Res.*, *117*, A08328, doi:10.1029/2012JA017632.

Li, J., S. A. Cummer, G. Lu, and L. Zigoneanu (2012), Charge moment change and lightning-driven electric fields associated with negative sprites and halos, *J. Geophys. Res.*, *117*, A09310, doi:10.1029/2012JA017731.

Liu, N. Y., and V. P. Pasko (2006), Effects of photoionization on similarity properties of streamers at various pressures in air, *J. Phys. D: Appl. Phys.*, *39*, 327–334, doi:10.1088/0022-3727/39/2/013.

Liu, N. Y., V. P. Pasko, K. Adams, H. C. Stenbaek-Nielsen, and M. G. McHarg (2009), Comparison of acceleration, expansion, and brightness of sprite streamers obtained from modeling and high-speed video observations, *J. Geophys. Res.*, *114*, A00E03, doi:10.1029/2008JA013720.

Luque, A., and U. Ebert (2010), Sprites in varying air density: Charge conservation, glowing negative trails and changing velocity, *Geophys. Res. Lett.*, *37*, L06806, doi:10.1029/2009GL041982.

McHarg, M. G., H. C. Stenbaek-Nielsen, and T. Kanmae (2007), Streamer development in sprites, *Geophys. Res. Lett.*, *34*, L06804, doi:10.1029/2006GL027854.

Morrow, R., and J. J. Lowke (1997), Streamer propagation in air, *J. Phys. D: Appl. Phys.*, *30*, 614–627.

Pasko, V. P., U. S. Inan, and T. F. Bell (1998), Spatial structure of sprites, *Geophys. Res. Lett.*, *25*, 2123–2126.

Pasko, V. P., Y. Yair, and C.-L. Kuo (2011), Lightning related transient luminous events at high altitude in the Earth's atmosphere: Phenomenology, mechanisms and effects, *Space Sci. Rev.*, 287, doi:10.1007/s11214-011-9813-9.

Qin, J., S. Celestin, and V. P. Pasko (2011), On the inception of streamers from sprite halo events produced by lightning discharges

with positive and negative polarity, *J. Geophys. Res.*, *116*, A06305, doi:10.1029/2010JA016366.

Qin, J., S. Celestin, and V. P. Pasko (2012a), Formation of single and double-headed streamers in sprite-halo events, *Geophys. Res. Lett.*, *39*, L05810, doi:10.1029/2012GL051088.

Qin, J., S. Celestin, and V. P. Pasko (2012b), Minimum charge moment change in positive and negative cloud to ground lightning discharges producing sprites, *Geophys. Res. Lett.*, *39*, L22801, doi:10.1029/2012GL053951.

Qin, J., S. Celestin, and V. P. Pasko (2013), Dependence of positive and negative sprite morphology on lightning characteristics and upper atmospheric ambient conditions, *J. Geophys. Res. Space Physics*, *118*, 2623–2638, doi:10.1029/2012JA017908.

Raizer, Y. P. (1991), *Gas Discharge Physics*, Springer-Verlag, New York, NY.

Stenbaek-Nielsen, H. C., and M. G. McHarg (2008), High time-resolution sprite imaging: Observations and implications, *J. Phys. D: Appl. Phys.*, *41*, 234009.

Stenbaek-Nielsen, H. C., D. R. Moudry, E. M. Wescott, D. D. Sentman, and F. T. S. Sabbas (2000), Sprites and possible mesospheric effects, *Geophys. Res. Lett.*, *27*, 3829–3832.

Stenbaek-Nielsen, H. C., R. Haaland, M. G. McHarg, B. A. Hensley, and T. Kanmae (2010), Sprite initiation altitude measured by triangulation, *J. Geophys. Res.*, *115*, A00E12, doi:10.1029/2009JA014543.

Suzuki, T., Y. Matsudo, T. Asano, M. Hayakawa, and K. Michimoto (2011), Meteorological and electrical aspects of several winter thunderstorms with sprites in the Hokuriku area of Japan, *J. Geophys. Res.*, *116*, D06205, doi:10.1029/2009JD013358.

van der Velde, O. A., A. Mika, S. Soula, C. Haldoupis, T. Neubert, and U. S. Inan (2006), Observations of the relationship between sprite morphology and in-cloud lightning processes, *J. Geophys. Res.*, *111*, D15203, doi:10.1029/2005JD006879.

Wait, J. R., and K. P. Spies (1964), Characteristics of the Earth-Ionosphere waveguide for VLF radio waves, *Tech Note 300*, National Bureau of Standards, Boulder, Colo.

Wescott, E. M., D. Sentman, M. Heavner, D. Hampton, W. A. Lyons, and T. Nelson (1998), Observations of 'Columniform' sprites, *J. Atmos. Sol. Terr. Phys.*, *60*, 733–740.

Zalesak, S. T. (1979), Fully multidimensional flux-corrected transport algorithms for fluids, *J. Comput. Phys.*, *31*, 335–362.